1 February 2002

ELSEVIER

Optics Communications 202 (2002) 47–54

OPTICS COMMUNICATIONS

www.elsevier.com/locate/optcom

Implementation of optical coherence tomography (OCT) in visualization of functional structures of cat visual cortex

R. Uma Maheswari[a], H. Takaoka[b], R. Homma[a], H. Kadono[c], M. Tanifuji[a,*]

[a] *Laboratory for Integrative Neural Systems, Brain Science Institute, RIKEN, 2-1 Hirosawa, Wako, Saitama, Japan*
[b] *Olympus Optical Co. Ltd., Japan*
[c] *Graduate School of Science and Engineering, Saitama University, Japan*

Received 2 August 2001; received in revised form 14 November 2001; accepted 21 November 2001

Abstract

We report the application of optical coherence tomography (OCT) for visualizing a 1D depth resolved functional structure of cat brain in vivo. The OCT system is based on the known fact that neural activation induces structural changes such as capillary dilation and cellular swelling. Detecting these changes as an amplitude change of the scattered light, an OCT signal reflecting neural activity, i.e., functional OCT (fOCT) could be obtained. Experiments have been done to obtain a depth resolved stimulus-specific profile of activation in cat visual cortex. © 2002 Published by Elsevier Science B.V.

1. Introduction

The brain is the most complex organ, and understanding its functional organization in correlation with its anatomical structures is of prime importance from both the clinical aspect and the fundamental aspect of how the brain orchestrates the various tasks simultaneously. Techniques such as functional magnetic resonance imaging (fMRI), positron emission tomography (PET) [1,2] provide volumetric functional images at a resolution of mm. However, the size of the functional unit consisting of neurons is a few tens of microns, thus requiring higher resolution.

The other technique is optical intrinsic signal imaging (OISI) [3–5] that visualizes neural activity induced changes of the reflected light from the cortical surface and could provide 2D functional map at a micron level resolution. It has also provided some valuable insights in understanding the function of the brain [4–8]. However in OISI, the reflected light is integrated over the depth and so the information about the organization with respect to the depth is lost. For example, the visual cortex consists of six layers as shown in Fig. 1 with the cellular responses of each layer not necessarily being the same: neurons in layers 2 and 3 selectively respond to a particularly oriented grating stimulus while layer 4 lacks such orientation selectivity [9]. In OISI, however, neural activity

* Corresponding author. Tel.: +81-48-462-1111; fax: +81-48-462-4696.
E-mail address: tanifuji@postman.riken.go.jp (M. Tanifuji).

0030-4018/02/$ - see front matter © 2002 Published by Elsevier Science B.V.
PII: S0030-4018(02)01079-9

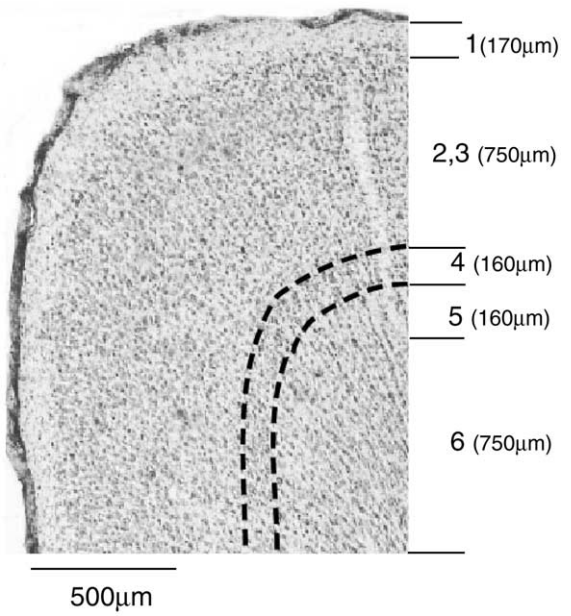

Fig. 1. Anatomical section of cat visual cortex. Although at first sight, it is difficult to detect the borders between the layers, a careful observation reveals the presence of the six-layered structure. Approximate values of the average thickness of the individual layers are indicated within brackets.

influenced signals are averaged over these layers. Further, as visible wavelengths are used, the penetration depth is limited to a few hundreds of microns.

The main purpose of the current study is to resolve the neural activity elicited signal along the layered structure by introducing the optical coherence tomographic (OCT) technique. In OCT, a low coherent light source in combination with an interferometer paves a way for selecting reflected light from a limited volume of specified depth [10]. OCT has been successfully employed in structural imaging of eye [10–12], skin [13], gastrointestinal tissues [14]. OCT has also been employed in imaging flow velocity [15,16]. However, its potential in mapping functional signals in the brain remains unexplored. Here, to our knowledge, for the first time OCT has been implemented for functional imaging of an intact brain.

Neural activation elicits secondary physiological changes such as: (i) a change in the cerebral blood volume which corresponds to a change in the capillary diameter [17,18]; (ii) a change in the density of red blood cells [19]; (iii) a decrease in extracellular volume which corresponds to the swelling of glial cells [20–22], that can give rise to scattering changes. As the signal measured in OCT is reflectivity, it varies with changes in the scattering characteristics. Therefore, it is theoretically possible to get a differential OCT signal reflecting changes elicited by neural activation. Current experiments have been done to test the feasibility of this method in one dimension. They present preliminary results with the main emphasis on verifying the existing knowledge of visual cortex [9,23].

2. Experiments

2.1. Experimental system

Fig. 2 shows the experimental system. It consists of a Mach–Zhender type interferometer constructed from single-mode fibers for flexibility [24]. Light from a broad-band light source (AFC Technologies, Canada) having a central mean wavelength of 1310 nm and a coherence length in free space of 30 μm is split into sample and reference beams in the respective ratio of 19:1 by coupler 1. The optical frequency of the reference signal is shifted to a 119.75 MHz by an acousto-optic modulator (AOM 1) while the frequency of the sample beam is shifted to a frequency 120 MHz by a second acousto-optic modulator (AOM 2). Interference of these signals results in a detected signal having a beat frequency of 250 kHz. Both the light beams with their frequencies shifted pass through the circulators to illuminate, respectively, the reference mirror and the cat cortex. The objective lens has a NA of 0.1 which will give a depth of focus 130 μm and a spot diameter of 16 μm. The reflected light from the cortex and the reference mirror are recombined at the coupler 2 in the respective ratio of 19:1. The polarization controllers (PC1–PC4) were used to maximize the output interference beat signal at the detector. Heterodyne detection was done with a lock-in amplifier locked to the beat frequency 250 kHz, and the amplitude of the beat signal is fed into the computer via a 16 bit A/D converter. The reference mirror M is

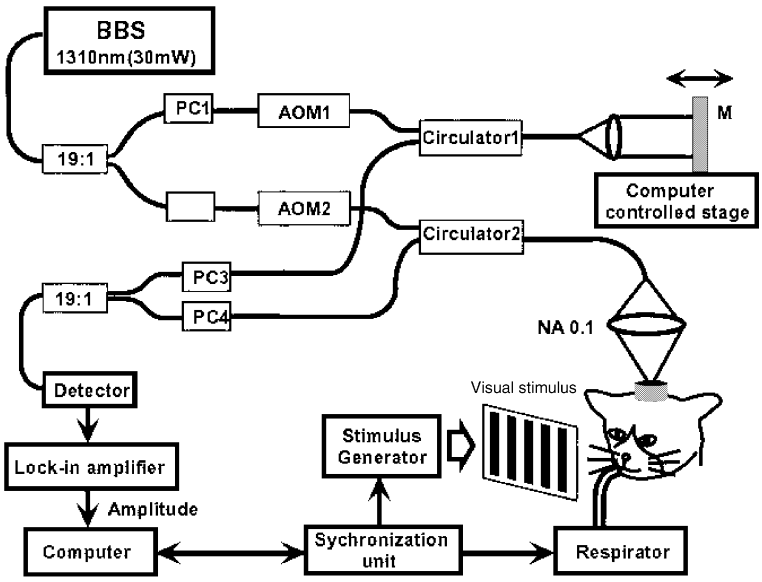

Fig. 2. Experimental system used to obtain a differential OCT signal from cat primary visual cortex.

mounted on a motorized stage moving at a speed of 2 mm/s corresponding to a frequency of 3 kHz well within the bandwidth of the lock-in amplifier.

To obtain the 1D depth resolved signal of the cortex, the reference mirror is scanned, and the reflectivity variations from different depths is recorded. Further, the probe unit consisting of fiber and objective lens is also attached with a CCD. The CCD is used to view the cortical surface in relation to the illuminating spot and is positioned to be at a plane conjugate to that of the fiber and the sample planes.

2.2. Experimental details

Experiments were performed on the exposed visual cortex of an anaesthetized cat. Anesthesia was maintained with a mixture of 70% N_2O and 30% O_2 supplemented with 1–2% isoflurane. The head of the animal was held tightly by attaching to a metal rod. A stainless steel chamber (18 mm inner diameter) was fixed onto the skull with dental acrylic cement by aseptic surgery and was placed above the skull. After careful removal of the skull and the dura matter which is the protective layer covering the cortex, the chamber was filled with 1.2% agarose (Agarose-HGS, Nacalai tesque, Japan Gel strength 1.5%) containing dexamethazone (0.1 mg/ml saline) and antibiotics (gentamicin, 0.25 mg/ml saline) and was sealed with a round glass cover slip and a silicon gasket. The exposed surface is shown in Fig. 3. After the procedure of chamber fixation and removal of dura matter, the animal was returned to the cage and a gap of around a week was given before OCT experiments for the cortex to recover from the metabolic changes due to exposure.

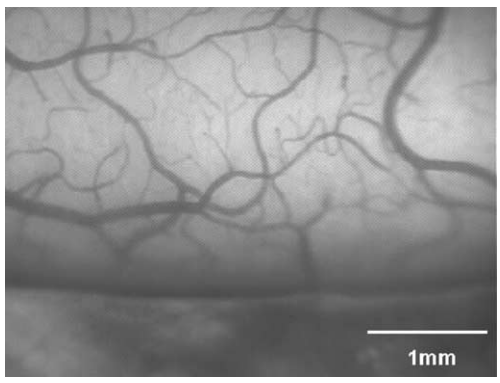

Fig. 3. Exposed cortical surface of a cat's visual cortex.

OCT experiments were carried out under the same anesthetic condition as that used during the surgery. Contact lenses were fitted to eyes to protect cornea from drying. The pupils of the eyes were dilated with 0.5% tropicamide and 0.5% phenylephrine hydrochroride. The center of the visual field was roughly estimated by projecting images of optic disks onto a screen in front of the animal. The distance of the CRT screen was adjusted to have the best focus of optic disks and surrounding vessel patterns and was around 20–30 cm from the animal's eyes. An image of the stimulus that has to be presented to the cat was shown on the CRT screen.

2.3. Stimulus and scan details

All visual stimuli were generated with a VSG2/3 graphics video board (Cambridge Research Systems, UK). The stimuli were square-wave gratings (white = 8 cd/m^2, black = 0 cd/m^2) having a spatial frequency 0.5 cycle/° and were moving at a velocity of 4 °/s. The grating stimuli were presented binocularly and shown in a sequential order. The presented grating stimulus activates neurons at the measuring site of the visual cortex when the orientation of the grating coincides with the optimal orientation of those neurons [9]. The stimulus set consists of four grating patterns namely, horizontal, vertical, diagonal left and diagonal right gratings. A blank screen corresponding to no stimulus case was used as control. The animal was artificially ventilated by a respirator unit. Its rectal temperature, ECG and expired CO_2 were continuously monitored during both OCT experiments and surgery.

In one trial, the reference mirror has been scanned back and forth over a period of 8 s with data acquisition starting 2 s prior to the onset of stimulus presentation. The duration of stimulus presentation is 2 s. A total of 16 scans, with four pre-stimulus scans and 12 post-stimulus scans had been done. An inter-stimulus interval of 5 s was given in between stimuli. A total of 40 such trials have been done for each stimulus and the average over those trials was calculated. The total number of averaging used was 240 and it corresponds to 40 trials times 6 scans. All data acquisition had been synchronized to the heartbeat and respiration of the cat.

The experimental protocol was approved by the Experimental Animal Committee of the RIKEN Institute. All experimental procedures were done in accordance with the guidelines of the RIKEN Institute and the National Institute of Health.

3. Results and discussion

3.1. OCT signal from cortex

Fig. 4 shows the averaged OCT reflectivity signals obtained when the focus was adjusted to a depth of around 300 μm below the surface as a function of the cortical depth d. Here the direction of the light beam was incident normal to the cortical surface. We can see two kinds of variation. The first one close to the surface displaying a sharp decay due to the difference in indices at the agarose–cortex interface. The peak position corresponding to surface of the cortex is fixed as the reference to be zero. The second one showing modulated variation is broad having many peaks

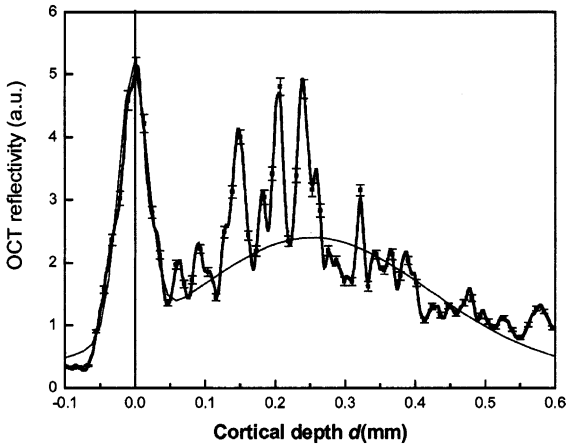

Fig. 4. Variation of the OCT signal as a function of cortical depth d (mm) when the light was focused to a point 300 μm below. The solid line shows the sum of the Gaussian profiles fitted to the sharp and broad variations. Sharp Gaussian has a width of 0.045 mm while the broad one has a width of 0.29 mm. The straight line drawn across the first peak is taken as the cortical surface and fixed as zero. Here error bars denote standard error of mean (SEM).

with the envelope of the peaks lying along the fitted Gaussian envelope. Now to interpret this component, we have to consider the effect of speckles that arise from multiple scattering within the illuminated volume of the tissue [25].

The single scans contain both the structural variations and the statistically independent dynamic speckles. However, due to temporal averaging by repeated scanning of the reference mirror as described in Section 2.3, the statistically independent speckles are averaged out. This was experimentally confirmed by comparing the averaged scan profile with that from a slightly shifted (around the average speckle diameter of 15 μm) lateral position and those two scan profiles were found to be almost identical. Therefore we can safely interpret the many peaked variations as the structural variations within the cortical tissue.

Comparing with Fig. 1, the measured averaged reflectivity variations are from layers 1 and 2/3. These averaged variations in the amplitude among the various peaks indicate the large differences existing within a layer and this could approximately correspond to both size of scattering centers that include neuron and glial cells, capillaries etc. within the measuring volume and local index variations.

When considering functional imaging, the following things become critical: (i) the height or the amplitude of the peaked variations has to be large enough over the noise level and (ii) the detectable change in the amplitude of these variations has to be larger than the noise level. In Fig. 4, error bars denote standard error of mean (SEM) obtained and it varies across the scanned depth. The change in the amplitude of the reflectivity variations from a certain depth has to be larger than SEM for that depth in order to contribute to the functional signal.

Here to calculate the cortical depth, a refractive index of 1.4 had been used. This value was calculated by moving the focus of the objective lens to deeper away from the surface as this would result in relative shift of the surface position in the OCT signal. From the physically moved distance in the sample arm and the actual shift in the OCT signal, refractive index of the tissue can be estimated [26]. This was estimated to be around 1.4 which agrees with the commonly assumed values of index for the brain [27].

3.2. Functional imaging

Now, the main interest lies in the second OCT signal component showing the peaked variations as they correspond to reflectivity variations from scattering inhomogeneities within the cortical layers. On neural activation, the question is, whether these reflectivity variations will show a definitive change elicited by neural activation. Theoretically, all the physiological structural changes such as capillary dilation, change in the density of red blood cells and swelling of glial cells taking place at a certain depth on neural activation would produce a finite change in the reflectivity of the OCT signal obtained from that depth. As this is expected to be small, careful measurement protocol would be needed that is described in Section 2.3.

3.2.1. Results of functional imaging

In order to quantify the functional signal obtained, we define the following:

Let the detected reflectivity at a cortical depth d and at time t for a stimulus s be $R_s(d,t)$ which results from scattering inhomogeneities present in the tissue. First, a ratio of the reflectivity at time t to that averaged over a period of 2 s corresponding to the initial four scans from the onset of data acquisition,

$$\gamma_s(d,t) = \frac{R_s(d,t)}{\sum_{\text{prescans}} R_s^{\text{pre}}(d,t)} \tag{1}$$

was calculated for all the grating stimuli and the control condition. The division operation in Eq. (1) removes the time-independent common variation and extracts only changes due to visual stimulation. Next, averaging was done over the 40 data sets to get $\langle \gamma_s(d,t) \rangle$ for each stimulus. From OISI studies, it has been shown that maximum change in the reflected light occurs during a period of approximately 1–3.5 s from the onset of stimulus [17]. Utilizing this fact, averaging the ratios obtained over this duration was calculated to be $\langle \gamma_s(d) \rangle$. Finally, the differential OCT signal $\langle \gamma_{\text{diff}}(d) \rangle$ was calculated as

$$\langle \gamma_{\text{diff}}(d) \rangle = \langle \gamma_{\text{grating}}(d) \rangle - \langle \gamma_{\text{blank}}(d) \rangle. \quad (2)$$

With the above equation, we estimated the change in reflectivity of the OCT signal due to a grating stimulus over the control condition. As this is a function of depth, it is possible to detect changes in depth direction with a resolution determined by the coherence length of the source.

Two examples obtained from two different animals shown in Figs. 5(a) and (b) demonstrate that a functional OCT or fOCT can indeed be realized and show the differential OCT signals $\langle \gamma_{\text{diff}}(d) \rangle$ obtained under two different stimuli namely horizontal and vertical grating as a function of the cortical depth d. The inset shows $\langle \gamma_{\text{diff}}(d) \rangle$ for all the grating stimuli in both (a) and (b). In both cases, the signal was well above the noise level determined by the error bars that correspond to SEM. We can infer the following facts from these figures:

1. In either case, across the whole scanned depth from 0 to 0.6 mm, there is a stimulus evoked change in the differential OCT signal $\langle \gamma_{\text{diff}}(d) \rangle$ and this change can be either positive of (0.25–0.55) mm for (a) and (0.2–0.45) mm for (b) or negative (0.05–0.25) mm for (a) and (0–0.19) mm for (b).
2. Over a depth range of (0.25–0.55) mm in case of (a), and (0.2–0.45) mm in case of (b), there is a orientation specific increase in $\langle \gamma_{\text{diff}}(d) \rangle$ with a relatively large increase seen for a particular oriented grating stimulus and here horizontal oriented grating.
3. Comparing the amplitudes of $\langle \gamma_{\text{diff}}(d) \rangle$ among all the four grating stimuli presented (insets), the amplitudes of $\langle \gamma_{\text{diff}}(d) \rangle$ for different stimuli do not differ largely over the depth range from 0 to 0.2 mm. Taking (2) also into account, the former region can be considered as relatively stimulus-less specific while the latter region can be considered as stimulus-specific.
4. Beyond 0.45 mm up to the measured depth of 0.6 mm, the difference in the amplitudes of $\langle \gamma_{\text{diff}}(d) \rangle$ among the stimuli is not large and again we can consider this region to be stimulus-less specific.

Now let us consider the implications of these above inferences in relation to the layered structure of the cortex shown in Fig. 1:

1. First of all we can see that the scanned depth of 0.6 mm covers most of layer 2/3 and possibly layer 4.
2. In the depth range from nearly 0.25 mm for (a), or 0.2 mm for (b) up to 0.45 mm where an increase in $\langle \gamma_{\text{diff}}(d) \rangle$ is observed overlaps with the layer 2/3. It is well known from single cell recording studies that cells in this layer respond to specific oriented grating stimulus and cells of

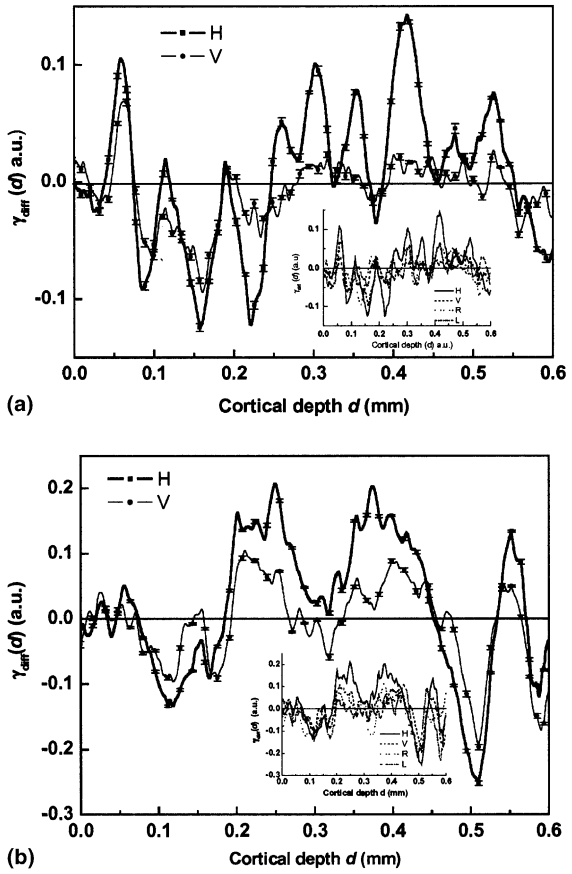

Fig. 5. Variation of the differential OCT signal $\langle \gamma_{\text{diff}}(d) \rangle$ as a function of the cortical depth d (mm) for horizontal and vertical grating stimuli from two different animals (a) and (b). The insets in both (a) and (b) show $\langle \gamma_{\text{diff}}(d) \rangle$ vs d for all the grating stimlui. In the figure H, V, R and L indicate horizontal, vertical, diagonal right and diagonal left grating stimuli. A moving averaging with a filter size of 40 μm approximately corresponding to the coherence length was done in all the curves shown here. Here error bars denote SEM. For clarity the error bars in the insets were removed.

similar preference are clustered together [9,24]. For the case of both (a) and (b) in Fig. 5, there is relatively a large increase in $\langle \gamma_{\text{diff}}(d) \rangle$ for the case of horizontal grating stimulus. This indicates that cells preferring horizontal grating are clustered together. So, our results agree well with the known fact.

3. From a depth of 0.075–0.25 mm for (a), and 0.05–0.2 mm for (b), falls into approximately layer 1. In this layer, we can see there are lesser number of scattering centers and hence in general there is less scattering. Further, as sensitive neurons are scarce in layer 1, there is only minimal activity resulting in decrease of $\langle \gamma_{\text{diff}}(d) \rangle$. One possible hypothesis to explain this feature could be the relative decrease in activity (for example in blood flow) in the upper layers to compensate for the requirement in the deeper region during activity.
4. The variation in the amplitude of $\langle \gamma_{\text{diff}}(d) \rangle$ with respect to orientation getting smaller beyond 0.45 mm indicates a partial loss in orientation specificity. Actually, this region gets closer to layer 4 where cells lack orientation specificity.

We know from OISI studies that the functional organization of the orientation selective cells in the direction parallel to the cortical surface consists of patches (called columns) with each column structure having a size around 500 μm [4]. However, the smallest size of the functional unit in the depth direction remains unknown. Actually, till now no organization across depth could be detected with the commonly employed electrophysiological studies mainly due to technical limitations. In Fig. 5, $\langle \gamma_{\text{diff}}(d) \rangle$ shows oscillatory variation for the horizontal grating stimulus. Here, the possibility of dynamic speckles arising from multiple scattering effects leading to such oscillatory variation can be excluded as the effect of speckles were greatly reduced by averaging and further the oscillatory variation is stimulus specific.

Therefore, we suggest this oscillatory variation may reflect a modular organization in depth too. The current system of fOCT is theoretically capable of resolving functional structures up to 30 μm in the depth direction assuming the source to be Gaussian. Approximating the oscillatory variation as the smallest functional unit that can be resolved by the proposed system, the width has been estimated to be 40 μm. This is one to two orders of magnitude high in comparison to the fMRI techniques.

The significant dependence of $\langle \gamma_{\text{diff}}(d) \rangle$ on stimulus reflects the potential of OCT in detecting neural activity-induced local scattering changes happening within a very small volume ($\approx 6000\ \mu m^3$). These local scattering changes could be the result of changes in the size of the cells or of change in the index variations or of density variations. In the examples shown, the cells along the depth direction have preference to the horizontal grating while being almost insensitive to other three grating orientations. We also found sites where amplitude of $\langle \gamma_{\text{diff}}(d) \rangle$ is large for a different orientation such as right diagonal grating with other orientations showing a smaller $\langle \gamma_{\text{diff}}(d) \rangle$ in the region supposed to be layer 2/3. These results demonstrate the reliability of stimulus specific changes of $\langle \gamma_{\text{diff}}(d) \rangle$.

4. Summary

OCT technique has been successfully employed to obtain a functionally dependent OCT signal called fOCT from an intact brain. Till now, to our knowledge, there has been no report about successful functional imaging of brain with OCT. A 1D depth resolved stimulus-specific profile has been obtained from cat visual cortex with an OCT system having a depth resolution of 30 μm which is much higher than that can be obtained by fMRI techniques. Improvements and modifications of the system have been going on to incorporate the possibility of x–y and x–z scans so that a 3D functional map at a lateral resolution of 50 μm and a depth resolution of 30 μm, much higher than the currently obtained ones could be realized.

Acknowledgements

We would like to thank Dr. Hongbin Li for his time in preparation of the anatomical sections. The first author was supported in part by Monbusho kakgakusho grant with grant no. 11750048.

References

[1] A.W. Toga, J.C. Mazziotta, Brain Mapping – The Methods, Academic press, New York, 1996.
[2] A. Villringer, U. Dirnagl, Cerebrovasc. Brain Metab. Rev. 7 (1995) 240.
[3] T. Bonhoeffer, A. Grinvald, J. Neurosci. 13 (1993) 4157.
[4] N. Uchida, Y. Takahashi, M. Tanifuji, K. Morii, Nature Neurosci. 3 (2000) 1035.
[5] G. Wang, K. Tanaka, M. Tanifuji, Science 272 (1996) 1665.
[6] D. Malonek, R.B.H. Tootell, A. Grinvald, Proc. Roy. Soc. London B 258 (1994) 109.
[7] G. Wang, M. Tanifuji, K. Tanaka, Neurosci. Res. 32 (1998) 33.
[8] K. Tsunoda, Y. Yamane, M. Tanifuji, Nature Neurosci. 4 (2001) 832.
[9] D.H. Hubel, T.N. Wiesel, J. Neurophysiol. 28 (1965) 229; D.H. Hubel, T.N. Wiesel, Ferrier lecture, Proc. Roy. Soc. London B 198 (1977) 1.
[10] D. Huang, E.A. Swanson, C.P. Lin, J.S. Schuman, W.G. Stinson, W. Chang, M.R. Hee, T. Flotte, K. Gregory, C.A. Puliafito, J.G. Fujimoto, Science 254 (1991) 1178.
[11] W. Drexler, U. Morgner, R.K. Ghanta, F.X. Kartner, J.S. Schuman, J.G. Fujimoto, Nature Med. 7 (2001) 502.
[12] S. Yazdanfar, A.M. Rollins, J.A. Izatt, Opt. Lett. 25 (2000) 1448.
[13] K.M. Yung, S.L. Lee, J.M. Schmitt, J. Biomed. Opt. 4 (1999) 125.
[14] A. Rollins, R. Ung-arunyawee, A. Chak, R.C.K. Wong, K. Kobayashi, M.V. Sivak, J.A. Izatt, Opt. Lett. 24 (1999) 1358.
[15] Y. Zhao, Z. Chen, C. Saxer, Q. Shen, S. Xiang, J.F. deBoer, J.S. Nelson, Opt. Lett. 25 (2000) 1358.
[16] M.D. Kulkarni, T.G. van Leeuwen, S. Yazdanfar, J.A. Izatt, Opt. Lett. 23 (1998) 1057.
[17] D. Malonek, A. Grinvald, Science 272 (1996) 551.
[18] M. Fukuda, M. Nishizaki, M. Tanifuji, Society for Neuroscience Abstracts 24, Poster no. 166.9, 1998, p. 426.
[19] M. Tomita, F. Gotoh, N. Tanahashi, P. Turcani, Am. J. Physiol. 251 (1986) H1205.
[20] P.G. Aitken, D. Fayuk, G.G. Somjen, D.A. Turner, METHODS: A comparison to methods in Enzymology 18 (1999) 91.
[21] K. Holthoff, O.W. Witte, J. Neurosci. 16 (1996) 2740.
[22] C. Nicholson, E. Sykova, TINS 21 (1998) 207.
[23] D.H. Hubel, Bye, Brain and Vision, Scientific American Library, New York, 1995.
[24] A.M. Rollins, J.A. Izatt, Opt. Lett. 24 (1999) 1484.
[25] J.M. Schmitt, S.H. Xiang, K.M. Yung, J. Biomed. Opt. 4 (1999) 95.
[26] G.J. Tearney, M.E. Berzinski, J.F. Southern, B.E. Bouma, M.R. Hee, T.G. Fujimoto, Opt. Lett. 20 (1995) 2258.
[27] B.C. Wilson, S.L. Jacques, IEEE J. Quantum Electron. 26 (1990) 2186.